Alzheimer's & Dementia®
THE JOURNAL OF THE ALZHEIMER'S ASSOCIATION

RESEARCH ARTICLE

Choroid plexus free-water correlates with glymphatic function in Alzheimer's disease

Xiaomeng Xu[1,2] | Xinyuan Yang[1] | Junfang Zhang[1,2] | Yan Wang[3] | Magdy Selim[4] |
Yingting Zheng[1] | Ruinan Shen[1] | Lipeng Sun[1] | Qi Huang[3] | Wenjing Wang[1] |
Wei Xu[1] | Yihui Guan[3] | Jun Liu[1] | Yulei Deng[1,2] | Fang Xie[3] | Binyin Li[1,2] |
the Alzheimer's Disease Neuroimaging Initiative (ADNI)

[1]Department of Neurology and Institute of Neurology, Ruijin Hospital, Shanghai Jiao Tong University School of Medicine, Shanghai, China

[2]Clinical Neuroscience Center, Ruijin Hospital LuWan Branch, Shanghai Jiao Tong University School of Medicine, Shanghai, China

[3]Department of Nuclear Medicine and PET Center, Huashan Hospital, Fudan University, Shanghai, China

[4]Stroke Division, Department of Neurology, Beth Israel Deaconess Medical Center, Harvard Medical School, Boston, Massachusetts, USA

Correspondence
Binyin Li, Department of Neurology and Institute of Neurology, Ruijin Hospital, Shanghai Jiao Tong University School of Medicine, 197 Ruijin Second Road, Shanghai 200025, China.
Email: libinyin@126.com

Fang Xie, Department of Nuclear Medicine and PET Center, Huashan Hospital, Fudan University, 518 East Wuzhong Road, Shanghai 200040, China.
Email: fangxie@fudan.edu.cn

The ADNI is detailed in Supplemental Acknowledgments.

FX and BL are co-corresponding authors. BL will handle correspondence at all stages of refereeing and publication, also post-publication

Abstract

INTRODUCTION: Free-water imaging of the choroid plexus (CP) may improve the evaluation of Alzheimer's disease (AD).

METHODS: Our study investigated the role of free-water fraction (FWf) of CP in AD among 216 participants (133 Aβ+ participants and 83 Aβ– controls) enrolled in the NeuroBank-Dementia cohort at Ruijin Hospital (RJNB-D). The Alzheimer's Disease Neuroimaging Initiative dataset was used for external validation.

RESULTS: At baseline, Aβ+ participants showed higher CP FWf, increased white matter hyperintensity (WMH) volume, and decreased diffusion tensor image analysis along the perivascular space (DTI-ALPS). In Aβ+ participants, DTI-ALPS mediated the association between CP FWf and periventricular WMH. CP FWf was associated with cortical tau accumulation, synaptic loss, hippocampal and cortical atrophy, and cognitive performance. During follow-up, CP FWf increased faster in Aβ+ participants than controls.

DISCUSSION: Elevated CP FWf indicated impaired glymphatic function and AD neurodegeneration, and can be a sensitive biomarker for AD progression. The study was registered on ClinicalTrials.gov (NCT05623124).

KEYWORDS
Alzheimer's disease, choroid plexus, diffusion tensor image analysis along the perivascular space, free-water mapping, white matter hyperintensity

Highlights

- This cohort study found higher free-water fraction (FWf) of the choroid plexus (CP) in amyloid beta (Aβ)+ participants.
- CP FWf was related to glymphatic function, brain atrophy, tau burden, synaptic loss, and cognition.
- Aβ+ participants showed faster growth of CP FWf than Aβ− controls during follow-up.
- The growth rate of CP FWf exceeded that of white matter lesion and tau accumulation in Aβ+ participants.
- CP FWf can serve as a sensitive imaging marker of glymphatic function and Alzheimer's disease progression.

1 | BACKGROUND

Alzheimer's disease (AD) is a neurodegenerative disorder marked by cognitive decline, amyloid beta (Aβ) plaques, hyperphosphorylated tau, and cortical atrophy.[1] Moreover, dysfunction in the cerebrospinal fluid (CSF) glymphatic clearance and white matter hyperintensities (WMHs) have also been identified as contributing factors.[2]

The choroid plexus (CP) produces CSF and regulates its dynamics.[3] Comprising a single-layer epithelium, fenestrated capillaries, connective tissue, and immune cells, the CP forms the blood–CSF barrier and aids immune surveillance.[3] However, the mechanisms behind the CP in neurodegeneration and AD are unclear. Despite this, there is a scarcity of research focusing on components of the CP. Given its role in producing CSF and its location within the ventricles, fluid is one of the predominant components within the CP structure.

Free water refers to unconstrained water molecules in fluid. Diffusion magnetic resonance imaging (MRI) techniques can measure free water in brain tissue.[4] A previous study showed increased free-water fraction (FWf) in cortical and subcortical regions as neurodegeneration progresses.[5] Given the CP's role in CSF regulation, CP FWf may be crucial for brain fluid circulation.

Furthermore, in the brain glymphatic system, CSF enters the brain parenchyma through the perivascular spaces surrounding arteries to clear interstitial fluid waste products.[6] Prior studies using diffusion tensor image analysis along the perivascular space (DTI-ALPS) index have shown an association between glymphatic dysfunction and the severity of WMHs.[7] Meanwhile, a previous study revealed an association between WMH and WMH-linked cortical AD biomarkers.[8] However, the relationship between CP FWf and glymphatic clearance or WMHs remains unclear.

We hypothesized that CP FWf in AD correlates with glymphatic function and neurodegeneration across the disease continuum. We undertook this study to: (1) investigate CP FWf changes in AD; (2) examine the relationships among CP FWf and glymphatic function, WMH, as well as AD pathological biomarkers; (3) explore potential mediation factors between CP FWf and cognition; and (4) validate the impact of CP FWf in AD using longitudinal data over a 12-month follow-up period.

2 | METHODS

2.1 | Participants and study design

This retrospective study used consecutive collected data from the Ruijin NeuroBank of Alzheimer's Disease and Dementia (RJNB-D) cohort between November 2021 and March 2024. The cohort is a prospective cohort for all-cause dementia from memory clinics and cognitively normal volunteers from the community, with detailed information in our previous study.[9]

The cross-sectional analysis included 216 participants: 133 Aβ+ individuals and 83 Aβ− controls. The Aβ+ group was further diagnosed as AD or mild cognitive impairment (MCI) according to 2016 National Institute on Aging–Alzheimer's Association criteria.[10] For longitudinal analysis, 76 of 216 baseline participants completed 12-month follow-up assessments, including repeated neuropsychological tests, multimodal MRI, and positron emission tomography (PET) scans. All follow-up assessments were conducted within 2 weeks of the 12-month interview.

For external validation, the Alzheimer's Disease Neuroimaging Initiative (ADNI) dataset was used. Participants continuously enrolled in ADNI 3 between June 2017 and June 2022 were included in the study. Apart from the ADNI enrollment criteria, the following additional exclusion criteria were applied: (1) without multi-shell diffusion MRI scans necessary for FWf calculation; (2) lack of 18F-florbetapir (FBP) PET scans required to determine Aβ status.

2.2 | Data collection

In RJNB-D, the participants underwent multimodal MRI, PET scans, neuropsychological tests, and blood sample collection (Figure S1A in

---

RESEARCH-IN-CONTEXT

1. **Systematic review**: The authors conducted a literature review using traditional sources, such as PubMed. Although free-water imaging of the choroid plexus (CP) has not been extensively studied, there is a growing research interest in the function of the CP. Several recent publications have explored the associations between the volumes of the CP, glymphatic function, cognition, and Alzheimer's disease (AD) pathology. These pertinent studies are appropriately cited in the article.

2. **Interpretation**: Our findings demonstrated that the free-water fraction (FWf) of the CP increased in individuals with AD pathology. Elevated CP FWf was associated with glymphatic dysfunction, brain atrophy, tau accumulation, synaptic loss, and cognitive decline. Additionally, a more rapid increase in CP FWf was observed in those with AD pathology.

3. **Future directions**: Prospective, longitudinal clinical and preclinical studies examining the features and functions of CP are needed to confirm the relationships among CP, glymphatic dysfunction, and neurodegeneration in AD.

---

supporting information). Multimodal MRI included 3D high-resolution T1, fluid-attenuated inversion recovery (FLAIR), multi-shell diffusion MRI (dMRI), and pseudo-continuous arterial spin labelled (pCASL) perfusion MRI (Figure S1B, Methods S1 in supporting information). PET scans included FBP for Aβ, ^{18}F-MK-6240 for tau, and ^{18}F-SynVesT-1 for synaptic density (Methods S2 in supporting information). Neuropsychological assessments included Mini-Mental State Examination (MMSE, Chinese Version),[11] 20 minute Auditory Verbal Learning Test (AVLT),[12] Clock-Drawing Test (CDT),[13] Boston Naming Test (BNT), Shape-Trail Test (STT-A and STT-B),[14] and animal fluency test (AFT).[14] Venous blood samples were used for apolipoprotein E (*APOE*) genotyping and glial fibrillary acidic protein (GFAP), neurofilament light chain (NfL), neurogranin (NRGN), and tumor necrosis factor-α (TNF-α; Methods S3 in supporting information).

2.3 | MRI acquisition and analysis

MRI data were acquired using a 3.0-T scanner with a 64-channel head coil (uMR 890, United Imaging Healthcare). Detailed parameters of T1-weighted, 3D FLAIR, diffusion, and pCASL sequences are presented in Methods S1.

Volumetric analysis was performed using FreeSurfer 7.1.1 (https://surfer.nmr.mgh.harvard.edu). WMHs were defined and segmented using Brain Intensity AbNormality Classification Algorithm (BIANCA, version 6.0, FMRIB Software Library), and further categorized into periventricular WMH (pWMH) and deep WMH (dWMH) by 10-mm

distance threshold from the ventricles.[8] Diffusion MRI data underwent pre-processing and tensor fitting to generate fractional anisotropy (FA) and mean diffusivity (MD), and to calculate DTI-ALPS index using FSL (version 6.0.3, http://www.fmrib.ox.ac.uk/fsl). Free-water imaging of CP was assessed using the neurite orientation dispersion and density imaging (NODDI) model. The CP FWf was calculated as the average of the left and right CP region of interest registered with T1-weighted image. Cerebral blood flow (CBF) in the CP was estimated using the FSL BASIL toolbox. Detailed information of MRI analysis is presented in Methods S1.

2.4 | PET MRI acquisition and analysis

The PET scans were performed using a 3T whole-body PET/MR scanner (uPMR 790, United Imaging). Participants received intravenous FBP for Aβ, ^{18}F-MK-6240 for tau, and ^{18}F-SynVesT-1 for synaptic vesicle glycoprotein 2A (SV2A) to assess synaptic loss as previously described.[15]

An automated pipeline derived cortical standardized uptake value ratios (SUVRs) using the PETSurfer toolbox in FreeSurfer 7.1.1 (https://surfer.nmr.mgh.harvard.edu), with the cerebellum as a reference. High-resolution segmentation from T1 images facilitated partial volume correction, followed by registration and validation of PET and anatomical images. Detailed information of PET MRI acquisition and analysis is presented in Methods S2.

2.5 | Statistical analyses

Group comparisons used *t* tests for continuous variables and chi-square tests for categorical variables. Non-normal distributions were log-transformed. Logistic regression was used to adjust for age, sex, and *APOE* genotype.

Within each group, correlations were assessed using Pearson or Spearman methods based on variable distribution. Multivariable linear regression analyzed CP FWf and other imaging measures, adjusted for age, sex, and *APOE* genotype. Vertex-wise correlation analysis using generalized linear model, controlled for age and sex, demonstrated spatial correlations between CP FWf and AD markers. Permutation tests reduced false positivity rates. Bonferroni correction addressed multiple comparisons. Mediation analyses were conducted using PROCESS v3.2 for SPSS (version 25.0, IBM), adjusted for age.

Longitudinal analysis was performed using repeated-measures analyses of variance. Alteration rates between Aβ+ participants and Aβ– controls were compared using a linear mixed model. The relationship between CP FWf and DTI-ALPS changes was explored in the Aβ+ group. Rates of longitudinal changes in CP FWf and related metrics were compared after standardizing baseline measures. Analyses were conducted using R (version 4.3.3, The R Foundation) or SPSS (version 25.0, IBM), with significance at *P* < 0.05 (two tailed). All analyses were independently performed by two authors (X.X. and X.Y.).

TABLE 1 Baseline demographic and MRI characteristics in RJNB-D cohort(n = 216).

	Aβ+ (n = 133)	Aβ− (n = 83)	p value
Age	70.59 ± 7.62	66.98 ± 8.13	0.001
Female	77 (58%)	51 (61%)	0.605
Education	11.56 ± 4.08	12.16 ± 3.43	0.266
APOE ε4 carrier[a]	67 (62%)	15 (23%)	<0.001
MMSE	21.07 ± 6.36	27.18 ± 4.02	<0.001
CP FWf	0.78 ± 0.04	0.76 ± 0.06	0.002
CPV	0.98 ± 0.20	0.94 ± 0.23	0.143
CP FA[b]	−1.65 ± 0.25	−1.64 ± 0.23	0.841
CP MD[b]	−7.64 ± 0.16	−7.67 ± 0.10	0.091
CP CBF[b]	3.80 ± 0.53	3.77 ± 0.85	0.746
DTI-ALPS	1.15 ± 0.17	1.23 ± 0.16	0.001
pWMH[b]	−3.83 ± 1.52	−4.78 ± 1.73	<0.001
dWMH[b]	−5.74 ± 1.70	−6.44 ± 1.73	0.005

Abbreviations: Aβ, amyloid beta; APOE, apolipoprotein E; CBF, cerebral blood flow; CP, choroid plexus; CPV, volume of choroid plexus; DTI-ALPS, diffusion tensor image analysis along the perivascular space; dWMH, deep white matter hyperintensity; FA, fractional anisotropy; FWf, free-water fraction; MD, mean diffusivity; MMSE, Mini-Mental State Examination; MRI, magnetic resonance imaging; pWMH, periventricular white matter hyperintensity; RJNB-D, NeuroBank-Dementia cohort at Ruijin Hospital.
[a]Different sample size for APOE genotype: Aβ+, n = 108; Aβ−, n = 66.
[b]The log-transformed values were used.

2.6 | Study approval

This study was approved by the ethics committee at Ruijin Hospital, Shanghai Jiao Tong University School of Medicine, China. All participants or caregivers provided written informed consent. The study adhered to the 1964 Declaration of Helsinki and its amendments. The study was registered on ClinicalTrials.gov (NCT05623124). Respectively, numbers of 94, 107, 120 participants of the same cohort overlapped previous publications,[8,9,15] regarding WMH-related neurodegeneration[8,15] and synaptic loss in AD.[9] This study furthered the previous findings by evaluating the influence of free water in the CP on glymphatic dysfunction and WMHs in AD.

3 | RESULTS

3.1 | Characteristics and group comparison

Table 1 summarizes the baseline characteristics of all participants from our RJNB-D cohort (n = 216, mean age, 69.20 years ± 8.00 [standard deviation (SD)]; 128 females). The Aβ+ group (n = 133) included Aβ+ MCI (n = 48) and AD (n = 85) and the Aβ− group (n = 83) consisted of cognitively unimpaired (CU, n = 64) and Aβ− MCI (n = 19). Table 2 lists the characteristics of the 76 participants who completed 12-month follow-up (mean age, 70.09 years ± 7.29 [SD]; 49 females).

TABLE 2 Month 12 demographic and MRI characteristics in RJNB-D cohort (n = 76).

|	Aβ+ (n = 46)	Aβ− (n = 30)	p value
Age	72.33 ± 6.22	66.67 ± 7.59	0.001
Female	28 (61%)	21 (70%)	0.416
APOE ε4 carrier[a]	27(63%)	5 (19%)	<0.001
Baseline CP FWf	0.77 ± 0.04	0.75 ± 0.05	0.020
Month 12 CP FWf	0.80 ± 0.04	0.76 ± 0.06	0.001
ΔCP FWf	0.03 ± 0.04	0.01 ± 0.04	0.046
Baseline DTI-ALPS	1.20 ± 0.14	1.27 ± 0.15	0.081
Month 12 DTI-ALPS	1.13 ± 0.18	1.23 ± 0.20	0.052
ΔDTI-ALPS	−0.08 ± 0.11	−0.05 ± 0.10	0.226
Baseline pWMH[b]	−4.01 ± 1.52	−4.83 ± 1.49	0.022
Month 12 pWMH[b]	−4.07 ± 2.20	−4.82 ± 1.96	0.126
ΔpWMH	0.01 ± 0.03	0.00 ± 0.01	0.078
Baseline tau SUVR[b]	0.64 ± 0.46	−0.03 ± 0.14	<0.001
Month 12 tau SUVR[b]	0.67 ± 0.51	−0.10 ± 0.16	<0.001
Baseline GFAP	153.05 ± 93.36	76.94 ± 64.01	<0.001
Month 12 GFAP	167.52 ± 84.90	128.61 ± 71.91	0.146

Abbreviations: Aβ, amyloid beta; APOE, apolipoprotein E; CP, choroid plexus; DTI-ALPS, diffusion tensor image analysis along the perivascular space; dWMH, deep white matter hyperintensity; FWf, free-water fraction; GFAP, glial fibrillary acidic protein; pWMH, periventricular white matter hyperintensity; RJNB-D, NeuroBank-Dementia cohort at Ruijin Hospital; SUVR, standardized uptake value ratio.
[a]Different sample size for APOE genotype: Aβ+, n = 43; Aβ−, n = 26.
[b]Nature logarithm was taken for normalization.

Compared to the Aβ− group, increased CP FWf (0.78 ± 0.04 vs. 0.76 ± 0.06, P = 0.002), pWMH volume (−3.83 ± 1.52 vs. −4.78 ± 1.73, P < 0.001), dWMH volume (−5.74 ± 1.70 vs. −5.74 ± 1.70, P = 0.005, both log transformed), and decreased DTI-ALPS (1.15 ± 0.17 vs. 1.23 ± 0.16, P = 0.001) were observed in Aβ+ participants (Table 1, Figure 1A). The FA, MD, CBF, and volumes of CP (CPV) were similar between groups (Table 1, all p > 0.050). A subgroup analysis of glymphatic markers between Aβ+ MCI and Aβ− MCI groups at similar cognitive stages showed no significant differences in CP FWf (0.77 ± 0.04 vs. 0.78 ± 0.04, p = 0.368), pWMH volume (−4.52 ± 1.61 vs. −4.52 ± 1.46, p = 0.990), dWMH volume (−6.05 ± 1.725 vs. −6.72 ± 1.857, p = 0.192), and DTI-ALPS (1.19 ± 0.18 vs. 1.19 ± 0.13, p = 0.984).

After adjustment for age, sex, and APOE genotype, CP FWf (β = 10.02, p = 0.015), DTI-ALPS (β = −3.19, p = 0.007), pWMH (β = 0.33, p = 0.007), and dWMH (β = 0.28, p = 0.013) independently indicated Aβ positivity (Tables S1–S4 in supporting information, respectively).
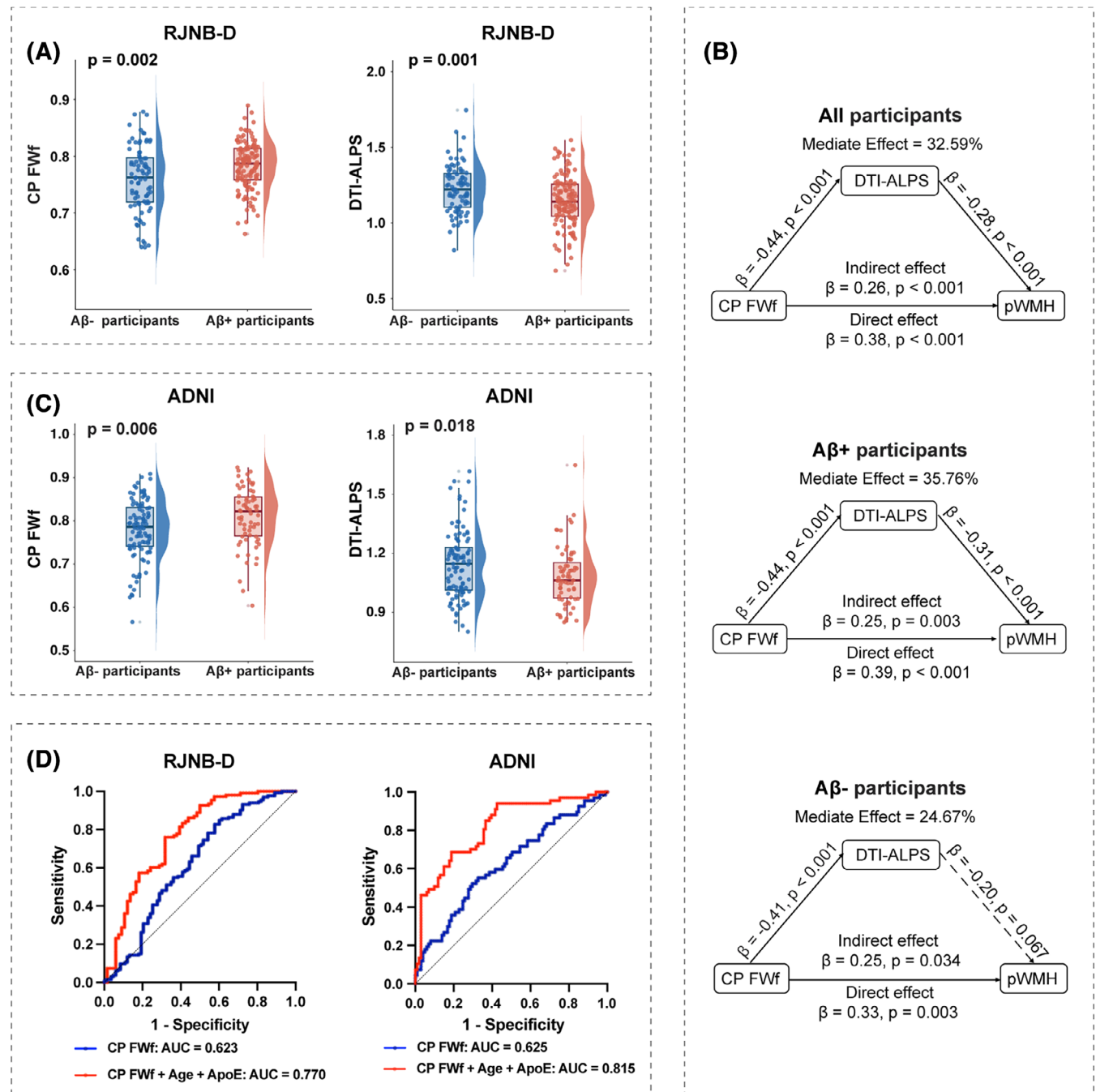
FIGURE 1 Group difference and correlation between CP FWf and glymphatic markers. A, Increased CP FWf ($p = 0.002$) and decreased DTI-ALPS ($p = 0.001$) were observed in Aβ+ participants in RJNB-D cohort. B, Across all participants, mediation analysis revealed a partial mediation effect of DTI-ALPS between CP FWf and pWMH. Within the Aβ+ group, a significant partial mediation effect of DTI-ALPS between CP FWf and pWMH was observed. The Aβ− controls displayed the trend of mediation effect of DTI-ALPS between CP FWf and pWMH. The log-transformed pWMH volume was used. All the mediation analysis was adjusted for age. C, Increased CP FWf ($p = 0.006$) and decreased DTI-ALPS ($p = 0.018$) were observed in Aβ+ participants in the ADNI dataset. D, Predictive values of CP FWf alone (blue) and with age and *APOE* genotype (red) for Aβ positivity calculated by ROC. The AUCs were similar for CP FWf alone (RJNB-D AUC = 0.623; ADNI: AUC = 0.625), and with age and *APOE* genotype (RJNB-D: AUC = 0.770; ADNI: AUC = 0.815). Aβ, amyloid beta; ADNI, Alzheimer's Disease Neuroimaging Initiative; AUC, area under the curve; *APOE*, apolipoprotein E; CP, choroid plexus; DTI-ALPS, diffusion tensor image analysis along the perivascular space; FWf, free-water fraction; pWMH, periventricular white matter hyperintensity; RJNB-D, NeuroBank-Dementia cohort at Ruijin Hospital; ROC, receiver operating characteristic.

3.2 | The CP FWf associated with DTI-ALPS and WMH

Among all participants, CP FWf correlated with DTI-ALPS ($r = -0.47$, $p < 0.001$), pWMH ($r = 0.46$, $p < 0.001$), and dWMH ($r = 0.21$, $p = 0.003$). With adjustment for age, mediation analysis showed DTI-ALPS partially mediated the association between CP FWf and pWMH (indirect effect standardized-$\beta = 0.26$, $p < 0.001$, mediated effect = 32.59%; Figure 1B), but not dWMH (indirect effect standardized-$\beta = 0.09$, $p = 0.236$).

Within the Aβ+ group, CP FWf correlated with DTI-ALPS ($r = -0.45$, $p < 0.001$) and pWMH ($r = 0.40$, $p < 0.001$), but not dWMH ($r = 0.11$, $p = 0.213$). Partial mediation effect of DTI-ALPS between CP FWf and pWMH was also observed (indirect effect standardized-$\beta = 0.25$, $p = 0.003$, mediated effect = 35.76%; Figure 1C), adjusted for age.

In Aβ− controls, CP FWf was also related to DTI-ALPS ($r = -0.44$, $p < 0.001$) and pWMH ($r = 0.45$, $p < 0.001$), yet the mediation effect of DTI-ALPS between CP FWf and pWMH was insignificant (Figure 1D), adjusted for age.

3.3 | Validation of CP FWf measurements

The measurements of CP FWf were repeated with an eroded CP mask (It shrunk the CP mask by 2mm in all directions using a box-shaped kernel) to minimize the contamination of CSF. The FWf in the eroded CP FWf was highly correlated with the original CP FWf ($\rho = 0.76$, $p < 0.001$), as well as DTI-ALPS ($\rho = -0.35$, $p < 0.001$) and pWMH ($\rho = 0.18$, $p = 0.044$, Figure S2 in supporting information). We also test the FWf measurement in another non-neuronal tissue: CSF. The distribution of FWf values in the central part of lateral ventricles was skewed, with the majority of values equaling 1 (Figure S3 in supporting information). It validated our application of FWf measurement because the main component of CSF in ventricles were free water.

External validation was further performed using the public ADNI dataset. Table S5 in supporting information summarizes the baseline characteristics of all participants ($n = 168$, mean age, 72.52 years ± 7.77 [SD]; 93 females). In the ADNI dataset, the Aβ+ group ($n = 67$) included CU ($n = 25$), MCI ($n = 31$), and AD ($n = 11$) and the Aβ− group ($n = 101$) consisted of CU ($n = 74$), MCI ($n = 26$), and dementia ($n = 1$). Consistent with our cohort, increased CP FWf (0.81 ± 0.07 vs. 0.78 ± 0.07, $p = 0.006$) and decreased DTI-ALPS (1.08 ± 0.15 vs. 1.14 ± 0.17, $p = 0.018$) were observed in Aβ+ participants from the ADNI dataset (Figure 1C). In the ADNI dataset, CP FWf was also highly correlated with DTI-ALPS among all the participants ($r = -0.53$, $p < 0.001$), in the Aβ+ subgroup ($r = -0.57$, $p < 0.001$), and in the Aβ− subgroup ($r = -0.48$, $p < 0.001$).

In addition, predictive values of CP FWf calculated by receiver operating characteristic was similar between ADNI (area under the curve [AUC] = 0.625) and our cohort (AUC = 0.623), and the predictive values were moderately improved when adjusted for age and *APOE* genotype (ADNI: AUC = 0.815; RJNB-D: AUC = 0.770, Figure 1D).

3.4 | CP FWf across the AD continuum

3.4.1 | CP FWf correlated with AD imaging and blood biomarkers

In the Aβ+ group of the RJNB-D cohort, CP FWf showed a significant relationship with AD imaging markers, including cortical tau SUVR, cortical SV2A SUVR, hippocampus volume, cortex volume, as well as MMSE score (Figure 2A, Table S6 in supporting information).

Adjusted for age, sex, and *APOE* genotype, elevated CP FWf linked to increased cortical tau accumulation (tau SUVR, $\beta = 9.27$, $p = 0.002$, Figure 2C, Table S7 in supporting information) and decreased cortical synaptic density (SV2A SUVR, $\beta = -3.43$, $p = 0.017$, Figure 2C, Table S8 in supporting information). However, CP FWf did not influence FBP SUVR ($\beta = 0.98$, $p = 0.103$). Vertex-wise analysis illustrated that CP FWf negatively correlated with cortical thickness in bilateral post cingulate gyrus, precuneus, temporal, and insular lobes, but positively correlated with tau SUVR in bilateral insular, temporal regions, and precuneus (Figure 2B). Moreover, CP FWf negatively correlated with SV2A SUVR in the right inferior parietal gyrus (Figure S4 in supporting information).

Within the Aβ+ group, CP FWf correlated with NfL ($\beta = 3.12$, $p = 0.026$, $n = 92$), GFAP ($\beta = 5.28$, $p < 0.001$, $n = 92$), NRGN ($\beta = 5.70$, $P = 0.028$, $n = 82$), and TNF-α ($\beta = 10.83$, $p = 0.009$, $n = 81$; Tables S9–S12 in supporting information), adjusted for age, sex, and *APOE* genotype. (Due to the different availability of adequate blood samples, the sample sizes are noted.)

Subgroup analysis (Aβ+ AD group and Aβ+ MCI group) was performed for each biomarker. As a result, the associations between CP FWf and SV2A SUVR, NfL, GFAP, NRGN remained significant in the AD stage (Figure 2C, red dashed line), whereas the associations between CP FWf and TNF-α were significant in the MCI stage (Figure 2C, green dashed line).

On the other hand, for the Aβ− group, the associations between CP FWf and biomarkers were also analyzed. Significant association was observed between CP FWf and tau SUVR ($\beta = 1.12$, $p = 0.025$) and TNF-α ($\beta = 9.15$, $p = 0.007$), but not SV2A SUVR ($\beta = -1.40$, $p = 0.121$), NfL ($\beta = 1.97$, $p = 0.090$), GFAP ($\beta = 1.24$, $p = 0.345$), or NRGN ($\beta = 4.12$, $p = 0.157$).

3.4.2 | AD biomarkers mediated CP FWf's effect on cognition

Increased CP FWf linked to worse cognitive performance, including overall cognition (MMSE, $\beta = -53.36$, $p < 0.001$), verbal function (AFT, $\beta = -29.83$, $p = 0.014$), and executive function (CDT, $\beta = -35.29$, $p = 0.025$) within the Aβ+ group (Figure 2C, Tables S13–S15 in supporting information), adjusted for age, sex, and *APOE* genotype.

Partial mediation effects of tau SUVR (indirect effect standardized-$\beta = -0.18$, $p = 0.043$, mediated effect = 40.88%, $n = 110$, Figure 3A), but not SV2A SUVR (indirect effect standardized-$\beta = -0.21$,

$p = 0.089$, mediated effect = 21.73%, $n = 64$, Figure 3B), was observed between CP FWf and MMSE, adjusted for age. Although NfL, NRGN, and TNF-α failed to mediate the association between CP FWf and MMSE (Figure 3D), GFAP exhibited a full mediation effect (mediated effect = 38.69%, $n = 111$, Figure 3C), adjusted for age. These findings suggested that the impact of CP FWf on cognition is mediated via tau- and GFAP-related pathways.

3.5 | The effect of longitudinal CP FWf changes

During the 12-month follow-up, CP FWf increased drastically in Aβ+ participants (F statistic = 16.673, corrected $p < 0.001$, Table S16 in supporting information). Moreover, Aβ+ participants demonstrated a faster growth rate than Aβ− controls (time × group interaction effect: F statistic = 4.118, corrected $p = 0.046$, Figure 4A, Table S16). The growth rates of CP FWf did not differ between APOE ε4 carriers ($n = 27$) and non-carriers ($n = 16$) in the Aβ+ group (F statistic = 0.004, $P = 0.949$, Figure 4B).
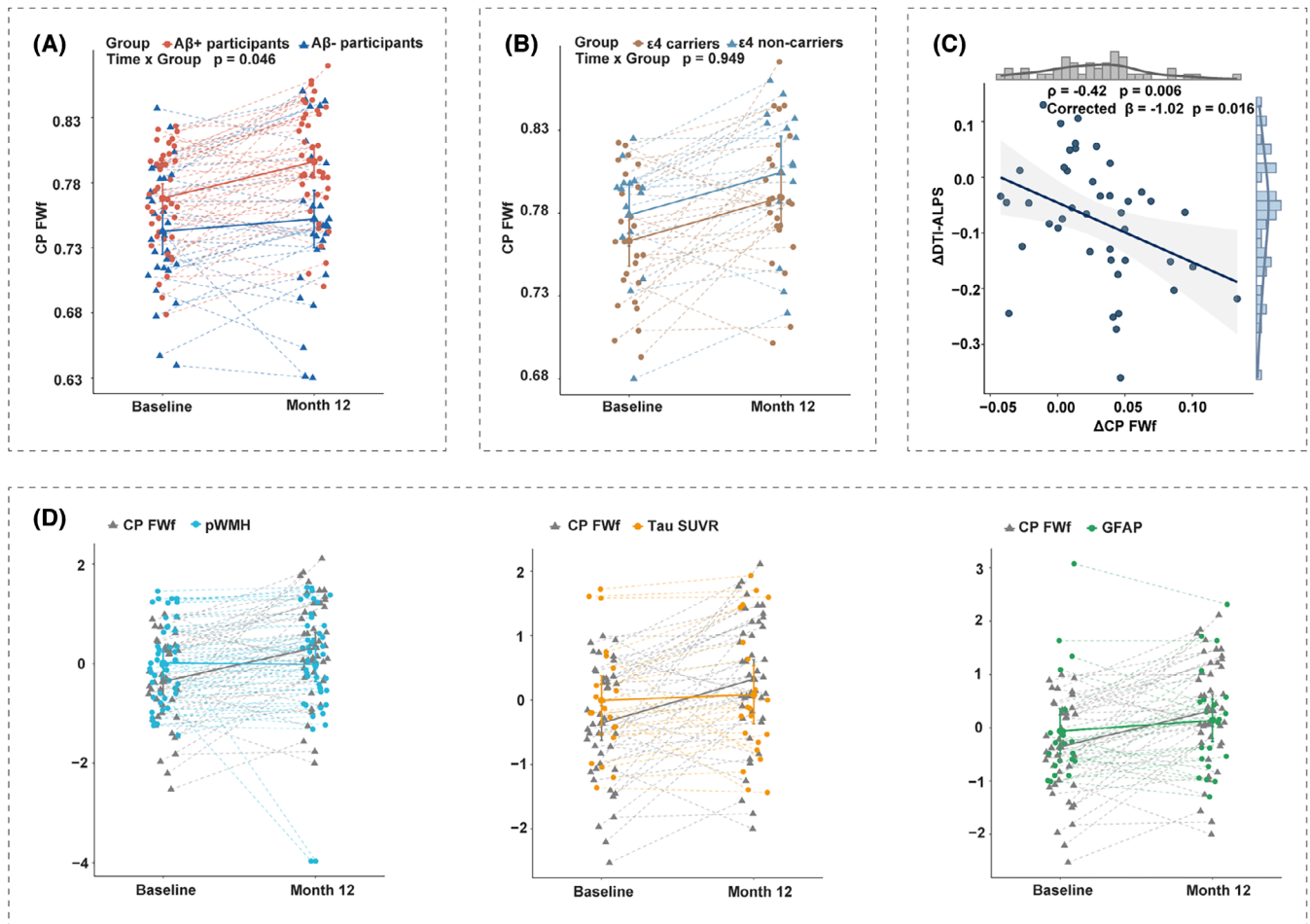
In Aβ+ participants, annual changes in CP FWf, DTI-ALPS, pWMH volume, and MMSE were calculated as ΔCP FWf, ΔDTI-ALPS, ΔpWMH, and ΔMMSE. Spearman correlation analysis suggested ΔCP FWf paralleled ΔDTI-ALPS ($\rho = -0.42$, $p = 0.006$, Figure 4C), but not ΔpWMH ($\rho = 0.21$, $p = 0.173$) or ΔMMSE ($\rho = -0.110$, $p = 0.482$). The association between ΔCP FWf and ΔDTI-ALPS remained significant upon adjustment for age and sex ($\beta = -1.02$, $p = 0.016$). The growth rate of CP

FIGURE 2 CP FWf correlated with imaging metrics and blood biomarkers in AD. A, Spearman correlation analysis between the potential imaging biomarkers of CP, glymphatic function markers, AD imaging markers, and global cognitive performance within the Aβ+ group. The CP FWf showed significant association with CP FA, CPV, DTI-ALPS, pWMH, cortical tau SUVR, cortical SV2A SUVR, hippocampus volume, cortex volume, and MMSE. The log-transformed pWMH volume was used. B, The vertex-wise GLM analysis revealed a negative correlation map between CP FWf and cortical thickness, and tau SUVR exhibited a positive correlation map with CP FWf. Age and sex were included as covariates in the GLM. Only the significant clusters with corrected $p < 0.05$ after permutations are colored. The color bar represents uncorrected vertex-wise p values. C, CP FWf correlated with peripheral blood AD biomarkers and cognition. Within the Aβ+ group, there was a positive correlation between CP FWf and NfL ($\beta = 3.117$, $p = 0.026$), GFAP ($\beta = 5.28$, $p < 0.001$), NRGN ($\beta = 5.70$, $p = 0.028$), TNF-α ($\beta = 10.83$, $p = 0.009$), and global tau ($\beta = 9.27$, $p = 0.002$). Subgroup analysis of AD (red) and MCI (green) stages were presented by dashed line. The log-transformed levels of blood AD biomarkers were used. Moreover, CP FWf was negatively associated with cognitive performance, including MMSE, AFT, and CDT and SV2A. All the regressions were adjusted for age, sex, and APOE genotype. Aβ, amyloid beta; AD, Alzheimer's disease; AFT, animal fluency test; APOE, apolipoprotein E; CBF, cerebral blood flow; CDT, Clock Drawing Test; CP, choroid plexus; CPV, volume of choroid plexus; DTI-ALPS, diffusion tensor image analysis along the perivascular space; FA, fractional anisotropy; FBP, 18F-florbetapir; FWf, free-water fraction; GFAP, glial fibrillary acidic protein; GLM, general linear model; MCI, mild cognitive impairment; MD, mean diffusivity; MMSE, Mini-Mental State Examination; NfL, neurofilament light chain; NRGN, neurogranin; pWMH, periventricular white matter hyperintensity; SUVR, standardized uptake value ratios; SV2A, synaptic vesicle glycoprotein 2A; TNF-α, tumor necrosis factor-α.
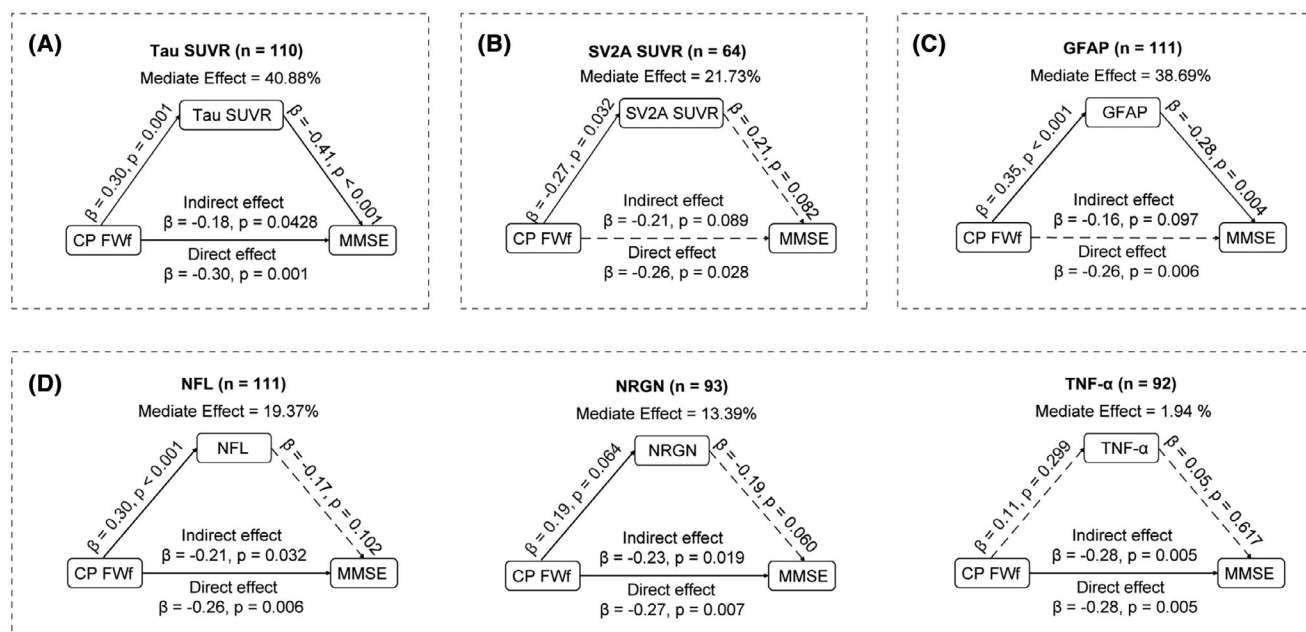
FIGURE 3 Mediation effects of AD biomarkers on the relationship between CP FWf and MMSE. We observed a partial mediation effect of tau (A), and marginal effect of SV2A (B). Notably, GFAP exhibited a full mediation effect (C). On the other hand, NfL, NRGN, and TNF-α did not significantly mediate the association between CP FWf and MMSE (D). All the mediation analysis was adjusted for age. AD, Alzheimer's disease; CP, choroid plexus; FWf, free-water fraction; GFAP, glial fibrillary acidic protein; MMSE, Mini-Mental State Examination; NfL, neurofilament light chain; NRGN, neurogranin; SUVR, standardized uptake value ratios; SV2A, synaptic vesicle glycoprotein 2A; TNF-α, tumor necrosis factor-α.

FIGURE 4 Longitudinal changes in CP FWf indicated neurodegeneration. The linear mixed model analysis indicated that Aβ+ participants exhibited a more rapid increase in CP FWf compared to Aβ− controls. Individual changes are represented by dashed lines, while the average changes in the group are depicted by solid lines (A). In the Aβ+ group, both *APOE ε4* carriers and non-carriers showed similar rates of CP FWf increase (B). The annual changes in CP FWf (ΔCP FWf) were significantly associated with alterations in DTI-ALPS (ΔDTI-ALPS) (C). Furthermore, linear mixed models with standardized preprocessing revealed that the growth rate of CP FWf surpassed that of pWMH, tau SUVR, and GFAP (D). Aβ, amyloid beta; *APOE*, apolipoprotein E; CP, choroid plexus; DTI-ALPS, diffusion tensor image analysis along the perivascular space; FWf, free-water fraction; GFAP, glial fibrillary acidic protein; pWMH, periventricular white matter hyperintensity; SUVR, standardized uptake value ratio.

FWf exceeded that of pWMH (interaction effect, *F* statistic = 11.201, corrected *p* = 0.001), tau SUVR (interaction effect, *F* statistic = 6.804, corrected *p* = 0.011) and GFAP (interaction effect, *F* statistic = 4.430, corrected *p* = 0.039, Figure 4D).

4 | DISCUSSION

Our study observed increased CP FWf and decreased DTI-ALPS index at baseline in Aβ+ participants. Also, we noted elevated CP FWf exacerbates pWMH, partially mediated by the glymphatic system, revealing a potential mechanism linking CSF dynamics to white matter lesions. We also observed significant associations between CP FWf and pivotal AD imaging markers (cortical tau SUVR, cortical SV2A SUVR, hippocampus volume, cortex volume) and cognitive performance. In longitudinal analyses, we observed a significant and faster increase in

CP FWf during a 12-month follow-up period in Aβ+ participants compared to Aβ− controls, and the rate of progression of CP FWf exceeded that of WMH and tau accumulation.

The CP is a highly vascularized structure that regulates CSF, clears neurotoxins, and plays a crucial role in the glymphatic system.[16,17] Studies in AD demonstrated that CPV was linked to cognitive impairment,[3,18–20] and levels of Aβ and tau in the CSF, indicating that CP may participate in the clearance of Aβ and tau.[18] Prior results regarding the relationship between CPV and Aβ positivity were inconsistent.[3,19,20] These disagreements may be attributed to the contamination of the partial volume effect of CSF in calculating CPV by traditional methods,[21] and also the morphological nature of CPV, which may display a relatively delayed response to Aβ deposition. Previous studies have demonstrated that CPV increased at a relatively late disease stage. Choi et al. analyzed CPV at different stages of AD in the disease spectrum, including early MCI, late MCI, and AD, and found

that CPV was greater in patients at late MCI and AD stages.[3] Similarly, using the ADNI dataset, Tadayon et al. divided the AD continuum into significant memory concern, early MCI, late MCI, and AD, and enlarged CPV was only observed in the AD stage.[18] The enlargement of CP is a chorionic morphological change, which may be due to a higher degree of stromal fibrosis, stromal dystrophic calcification, blood vessel thickening, or inflammation.[3] Therefore, the change of CPV may be detected at delayed disease stages. In the current study, we view the AD continuum as a whole disease spectrum without manually dividing the disease stages, and we also failed to verify the association between CPV and Aβ positivity. However, after evaluating various novel imaging biomarkers that reflect CP microstructure, including CP FWf, CP FA, CP MD, and CP CBF, we found that CP FWf, derived from free-water mapping, was the only index that significantly differed between Aβ+ and Aβ− groups. Free-water mapping uses a bi-tensor model to differentiate water diffusion in brain tissue and extracellular space, providing better microstructural insights than the traditional single-tensor model.[22,23]

The DTI-ALPS index is a reliable parameter of the glymphatic system.[24] Previous studies showed that enlarged CP and reduced DTI-ALPS were both associated with WMH growth.[7,19] Moreover, DTI-ALPS mediated the association between CP and WMH burden, suggesting that WMH growth can result from glymphatic disorder.[7] In our study, CP FWf showed solid correlation with DTI-ALPS and WMHs, suggesting that CP FWf reliably indicated glymphatic function. We noticed that in Aβ+ participants CP FWf was associated with pWMH that were anatomically located nearer to the CP, but not with dWMH, and there is a partial mediating effect of DTI-ALPS between CP FWf and pWMH.

A recent study by Jeong et al. demonstrated a positive correlation between CP enlargement and Aβ burden, but this correlation was only significant in the AD non-dementia group,[20] likely due to the "ceiling effect," as Aβ is saturated in the dementia state.[25] Similarly, our study showed that CP FWf was significantly associated with Aβ positivity, but did not correlate with Aβ burden measured by FBP SUVR. Additionally, our subgroup analysis comparing Aβ+ MCI and Aβ− MCI groups did not reveal significant differences in CP FWf, WMH, or DTI-ALPS. These findings suggest that CP FWf is primarily involved in non-specific neurodegeneration rather than Aβ pathology. However, due to the limited sample size of our Aβ− MCI group, future studies should further investigate the relationship between CP FWf and non-AD dementias.

A recent report indicated a positive correlation between global tau burden and CP enlargement in AD.[26] We further these findings by vertex-wise analysis, and showed that CP FWf changed in parallel with tau accumulation primarily in bilateral insular, temporal lobes, and precuneus. Furthermore, we found that increased tau burden mediated the detrimental effects of CP FWf on cognition. This finding adds clinical evidence to a recent study indicating that glymphatic dysfunction impairs cognition through poor tau clearance in AD mouse models.[27]

In addition to the clearance of neurotoxins, the glymphatic system can also modulate neuroinflammation.[28] We investigated the relationship between AD-related markers and CP FWf in the Aβ+ group through a subgroup analysis (AD and MCI). The results showed that CP FWf was significantly associated with NfL, GFAP, and NRGN in

the AD stage, while its association with TNF-α was significant in the MCI stage. However, when considering the disease continuum within the A-T-N framework (combining AD and MCI individuals with the same Aβ+ pathological background) CP FWf exhibited significant associations with all biomarkers, including tau, SV2A, NfL, GFAP, NRGN, and TNF-α. Among them, GFAP correlated with CP FWf, and substantially mediated the negative impact of CP FWf on cognitive function. GFAP is a structural protein in astrocytes and is a marker of astrocyte activation related to aging.[29] A previous study using a PET tracer of astrocyte reactivity has further confirmed the activation of astrocytes in AD and late-onset cognitive decline.[30] And recent study showed that blood GFAP correlated to impaired glymphatic function and global cognition in community-dwelling older adults.[31] Astrocytes are critical components of the glymphatic system by ensheathing the brain vasculature with their endfeet.[6,28] Through the aquaporin-4 (AQP4) channels enriched on their endfeet, astrocytes actively participate in the regulation of glymphatic function and the clearance of metabolic waste, such as Aβ and tau.[32] The location of astrocytic AQP4 is under dynamic regulation. In the state of neurodegeneration, astrocyte activation and AQP4 mislocation was observed, and may affect the glymphatic clearance of Aβ and tau.[32] Our findings, consistent with the previous publications, provided new evidence for involvement of an astrocyte-related pathway in glymphatic dysfunction in AD pathology.

We have also performed an association analysis between CP FWf and biomarkers in the Aβ− group. Significant association was observed between CP FWf and tau SUVR and TNF-α. Combined with the findings in the Aβ+ group, the results suggested that tau and neuroinflammation may be potential mechanisms underlying CP FWf alterations in the progress of neurodegeneration. However, the exact and detailed mechanisms need further experimental and clinical evidence.

The current study is the first to calculate the FWf of CP. To further validate the solidity of our measurements, the FWf values of non-neuronal free water in lateral ventricles and eroded part of CP were extracted. Consistent with our expectations, the FWf of CSF in the lateral ventricles was approximate to 1, and the FWf of eroded CP was highly correlated to CP. Finally, the diagnostic power (AUC) of CP FWf was highly consistent in ADNI and our cohort. Although as a single parameter the CP FWf failed to present optimal AUCs, the values were moderately improved with adjustment of age and *APOE* genotype, indicating its potential value as one of the contributors in a composite predictive frame.

Our study is aimed at providing a novel imaging marker for glymphatic function. In addition to traditional glymphatic markers, CP FWf provided microstructural insights about the CP. In the AD continuum, CP FWf, but not DTI-ALPS, WMH, or CPV, is related to tau and SV2A (Figure 2A). Our findings suggested that CP FWf may be related to multiple mechanisms of AD progression and neurodegeneration. Combined with traditional glymphatic markers like DTI-ALPS, WMH, and CPV, we hope that CP FWf can assist the non-invasive evaluation of glymphatic function in neurodegenerative conditions like AD.

Our study has limitations. First, the sample size of this longitudinal study is small, as the cohort is newly established with approximately half of the participants not reaching the 12-month follow-up. Also,

this duration may be too short to observe significant changes in cognitive performance and imaging markers like pWMH volume, suggesting a longer follow-up is warranted. However, ΔCP FWf already showed remarkable changes, indicating its sensitivity in monitoring disease progression. Additionally, the limited number of blood samples and analyses may influence the results, so findings related to blood markers should be viewed as exploratory and hypothesis generating.

In conclusion, our results indicate that CP FWF serves as a novel imaging marker that reflects various neurodegenerative features in AD, complementing structural MRI and PET imaging. By capturing the multifaceted aspects and longitudinal changes in AD, CP FWF holds potential for monitoring of disease progression, offering the possibility of personalized and timely treatment interventions.

CONFLICT OF INTEREST STATEMENT

Fang Xie is an associate editor of *Alzheimer's & Dementia*. Other authors declare no conflicts of interest. Author disclosures are available in the supporting information.

DATA AVAILABILITY STATEMENT

For all main figures with RJNB-D datasets, the extracted traces from the raw image files are available on Figshare (https://figshare.com/articles/dataset/Choroid_Plexus_Free-Water_Correlates_with_Glymphatic_Dysfunction_and_Tracks_Neurodegeneration_in_Alzheimer_s_Disease_The_RJNB-D_Study/26043871). Values for all data points in graphs are reported in the Supporting Data Values file.

The preprocessing codes for multimodal MR and PET are available as a Github repository (https://github.com/colorfulbrain/CP_FWf). The R/SPSS code used for the main analysis are available from the corresponding author upon request.

CONSENT STATEMENT

All human subjects provided informed consent.

ORCID

Xiaomeng Xu https://orcid.org/0000-0002-1717-538X

Binyin Li https://orcid.org/0000-0002-7903-2149

REFERENCES

1. Jack CR, Bennett DA, Blennow K, et al. A/T/N: an unbiased descriptive classification scheme for Alzheimer disease biomarkers. *Neurology*. 2016;87(5):539-547. doi:10.1212/WNL.0000000000002923

2. Garnier-Crussard A, Cotton F, Krolak-Salmon P, Chételat G. White matter hyperintensities in Alzheimer's disease: beyond vascular contribution. *Alzheimers Dement*. 2023;19(8):3738-3748. doi:10.1002/alz.13057

3. Choi JD, Moon Y, Kim HJ, Yim Y, Lee S, Moon WJ. Choroid Plexus Volume and Permeability at Brain MRI within the Alzheimer Disease Clinical Spectrum. *Radiology*. 2022;304(3):635-645. doi:10.1148/radiol.212400

4. Wang Y, Wang Q, Haldar JP, et al. Quantification of increased cellularity during inflammatory demyelination. *Brain*. 2011;134(Pt 12):3590-3601. doi:10.1093/brain/awr307

5. Chiu SY, Chen R, Wang WE, et al. Longitudinal Free-Water Changes in Dementia with Lewy Bodies. *Mov Disord*. 2024;39(5):836-846. doi:10.1002/mds.29763

6. Hablitz LM, Nedergaard M. The glymphatic system. *Curr Biol*. 2021;31(20):R1371-R1375. doi:10.1016/j.cub.2021.08.026

7. Li Y, Zhou Y, Zhong W, et al. Choroid Plexus Enlargement Exacerbates White Matter Hyperintensity Growth through Glymphatic Impairment. *Ann Neurol*. 2023;94(1):182-195. doi:10.1002/ana.26648

8. Zhang J, Chen H, Wang J, et al. Linking white matter hyperintensities to regional cortical thinning, amyloid deposition, and synaptic density loss in Alzheimer's disease. *Alzheimers Dement*. 2024;20(6):3931-3942. doi:10.1002/alz.13845. Published online April 22, 2024.

9. Li B, Chen H, Zheng Y, et al. Loss of synaptic density in nucleus basalis of meynert indicates distinct neurodegeneration in Alzheimer's disease: the RJNB-D study. *Eur J Nucl Med Mol Imaging*. 2024;52(1):134-144. doi:10.1007/s00259-024-06862-z. Published online August 8, 2024.

10. Cummings J. The National Institute on Aging-Alzheimer's Association Framework on Alzheimer's disease: application to clinical trials. *Alzheimers Dement*. 2019;15(1):172-178. doi:10.1016/j.jalz.2018.05.006

11. Katzman R, Zhang MY, null Ouang-Ya-Qu, et al. A Chinese version of the Mini-Mental State Examination; impact of illiteracy in a Shanghai dementia survey. *J Clin Epidemiol*. 1988;41(10):971-978. doi:10.1016/0895-4356(88)90034-0

12. Zhao Q, Lv Y, Zhou Y, Hong Z, Guo Q. Short-term delayed recall of auditory verbal learning test is equivalent to long-term delayed recall for identifying amnestic mild cognitive impairment. *PLoS One*. 2012;7(12):e51157. doi:10.1371/journal.pone.0051157

13. Mendez MF, Ala T, Underwood KL. Development of scoring criteria for the clock drawing task in Alzheimer's disease. *J Am Geriatr Soc*. 1992;40(11):1095-1099. doi:10.1111/j.1532-5415.1992.tb01796.x

14. Zhao Q, Guo Q, Hong Z. Clustering and switching during a semantic verbal fluency test contribute to differential diagnosis of cognitive impairment. *Neurosci Bull*. 2013;29(1):75-82. doi:10.1007/s12264-013-1301-7

15. Zhang J, Wang J, Xu X, et al. In vivo synaptic density loss correlates with impaired functional and related structural connectivity in Alzheimer's disease. *J Cereb Blood Flow Metab*. 2023;43(6):977-988. doi:10.1177/0271678X231153730

16. Dai Z, Yang Z, Chen X, et al. The aging of glymphatic system in human brain and its correlation with brain charts and neuropsychological functioning. *Cereb Cortex*. 2023;33(12):7896-7903. doi:10.1093/cercor/bhad086

17. Čarna M, Onyango IG, Katina S, et al. Pathogenesis of Alzheimer's disease: involvement of the choroid plexus. *Alzheimer's & Dementia*. 2023;19(8):3537-3554. doi:10.1002/alz.12970

18. Tadayon E, Pascual-Leone A, Press D, Santarnecchi E, Alzheimer's Disease Neuroimaging Initiative. Choroid plexus volume is associated with levels of CSF proteins: relevance for Alzheimer's and

Parkinson's disease. *Neurobiol Aging*. 2020;89:108-117. doi:10.1016/j.neurobiolaging.2020.01.005

19. Hong H, Hong L, Luo X, et al. The relationship between amyloid pathology, cerebral small vessel disease, glymphatic dysfunction, and cognition: a study based on Alzheimer's disease continuum participants. *Alzheimers Res Ther*. 2024;16(1):43. doi:10.1186/s13195-024-01407-w

20. Jeong SH, Park CJ, Cha J, et al. Choroid Plexus Volume, Amyloid Burden, and Cognition in the Alzheimer's Disease Continuum. *Aging Dis*. 2024;16(1):552-564. doi:10.14336/AD.2024.0118. Published online January 23, 2024.

21. Saito Y, Kamagata K, Uchida W, Takabayashi K, Aoki S. The partial volume effect of choroid plexus in pathogenesis of Alzheimer's disease. *Alzheimer's & Dementia*. 2023;19(10):4756-4757. doi:10.1002/alz.13123

22. Pasternak O, Sochen N, Gur Y, Intrator N, Assaf Y. Free water elimination and mapping from diffusion MRI. *Magn Reson Med*. 2009;62(3):717-730. doi:10.1002/mrm.22055

23. Zhou L, Li G, Zhang Y, et al. Increased free water in the substantia nigra in idiopathic REM sleep behaviour disorder. *Brain*. 2021;144(5):1488-1497. doi:10.1093/brain/awab039

24. Butler T, Zhou L, Ozsahin I, et al. Glymphatic clearance estimated using diffusion tensor imaging along perivascular spaces is reduced after traumatic brain injury and correlates with plasma neurofilament light, a biomarker of injury severity. *Brain Commun*. 2023;5(3):fcad134. doi:10.1093/braincomms/fcad134

25. Bjorkli C, Sandvig A, Sandvig I. Bridging the Gap Between Fluid Biomarkers for Alzheimer's Disease, Model Systems, and Patients. *Front Aging Neurosci*. 2020;12:272. doi:10.3389/fnagi.2020.00272

26. Ota M, Sato N, Nakaya M, et al. Relationship between the tau protein and choroid plexus volume in Alzheimer's disease. *Neuroreport*. 2023;34(11):546-550. doi:10.1097/WNR.0000000000001923

27. Lopes DM, Wells JA, Ma D, et al. Glymphatic inhibition exacerbates tau propagation in an Alzheimer's disease model. *Alzheimer's Research & Therapy*. 2024;16(1):71. doi:10.1186/s13195-024-01439-2

28. Mogensen FLH, Delle C, Nedergaard M. The Glymphatic System (En)during Inflammation. *Int J Mol Sci*. 2021;22(14):7491. doi:10.3390/ijms22147491

29. Sabbatini M, Barili P, Bronzetti E, Zaccheo D, Amenta F. Age-related changes of glial fibrillary acidic protein immunoreactive astrocytes in the rat cerebellar cortex. *Mech Ageing Dev*. 1999;108(2):165-172. doi:10.1016/s0047-6374(99)00008-1

30. Calsolaro V, Matthews PM, Donat CK, et al. Astrocyte reactivity with late-onset cognitive impairment assessed in vivo using 11C-BU99008 PET and its relationship with amyloid load. *Mol Psychiatry*. 2021;26(10):5848-5855. doi:10.1038/s41380-021-01193-z

31. Wei YC, Hsu CCH, Huang WY, et al. Vascular risk factors and astrocytic marker for the glymphatic system activity. *Radiol Med*. 2023;128(9):1148-1161. doi:10.1007/s11547-023-01675-w

32. Das N, Dhamija R, Sarkar S. The role of astrocytes in the glymphatic network: a narrative review. *Metab Brain Dis*. 2024;39(3):453-465. doi:10.1007/s11011-023-01327-y

SUPPORTING INFORMATION

Additional supporting information can be found online in the Supporting Information section at the end of this article.